Journal of Nuclear Materials 604 (2025) 155495

Contents lists available at ScienceDirect

Journal of Nuclear Materials

journal homepage: www.elsevier.com/locate/jnucmat

On the product phases and the reaction kinetics of carbothermic reduction of UO_2+C at relatively low temperatures

Chinthaka M. Silva [a,c,*], Kyle J. Kondrat [a,b], Bradley C. Childs [a], Maryline G. Ferrier [a], Michelle M. Greenough [a], Kiel S. Holliday [a], Scott J. McCormack [b]

[a] Lawrence Livermore National Laboratory, Livermore, CA 94550, USA
[b] Department of Materials Science and Engineering, University of California, Davis, CA 95616, USA
[c] Currently Affiliated with Pacific Northwest National Laboratory, Richland, WA 99354, USA

ARTICLE INFO

Keywords:
Uranium monocarbide
Carbothermic reduction
Nuclear fuel

ABSTRACT

The synthesis of UC using carbothermic reduction of UO_2 and C mixtures has been well studied at high temperatures. However, the product phase behavior of carbothermic reduction at low temperatures (≤1773 K) is not well studied. Such a study is important as low temperatures permit single phase UC synthesis without forming secondary higher carbides, and it further supports the knowledge base of the process that needs to be used for transuranic elements such as plutonium that have high vapor pressures at elevated temperatures. Therefore, a low temperature carbothermic reduction of two different C/UO_2 molar ratios under inert and reducing environments have been studied here. Two different sample holding crucibles, alumina (Al_2O_3) and graphite, were also used here to differentiate the hypostoichiometric (UC_{1-a}) and oxygen dissolved ($UC_{1-x}O_x$) uranium monocarbide phases adding more details on the two systems. Also, the reaction kinetics involved in the formation of UC via the carbothermic reduction of UO_2+C using product phases instead of evolved gases such as carbon monoxide is reported here. Under inert atmospheres but with significant oxygen partial pressures, the low temperature carbothermic reduction of UO_2+C produced up to 90 wt.% $UC_{1-x}O_x$ type oxycarbides as was confirmed by Xray powder diffraction. Reducing Ar-4%H_2 environments at these temperatures were not successful in synthesizing UC as it reduces the amount of C required for the carbothermic reduction, leaving UC phase at a non-equilibrium state. Inert atmospheres with low or negligible oxygen partial pressures on the other hand produced near stoichiometric UC at high phase purity, especially at 1673 – 1773 K temperature range. An activation energy of 377±75 kJmol^{-1} was also calculated using product phase concentrations of the carbothermic reduction of UO_2+C under these inert $Ar_{(g)}$ atmospheres.

1. Introduction

Studies have been conducted for decades to identify alternative nuclear fuels to that of the conventional uranium oxide (UO_2) for the next generation nuclear reactors. Even though uranium monocarbide (UC) in its original form is not a desirable fuel for aqueous nuclear reactors as it has greater reactivity with oxygen or air compared to UO_2 [1], it can be considered as one of the nuclear fuel candidates for non-aqueous nuclear reactors such as the Generation-IV gas-cooled fast reactor (GFR), lead-cooled fast reactor (LFR), and sodium-cooled fast reactor (SFR) due to its favorable chemical, physical, and neutronic properties [2–4], UC has a high melting point (2663±293 K) and phase stability at preferable temperatures similar to UO_2 [4,5], while it also has a higher thermal conductivity [3,4] and a higher fissile metal density than UO_2. In addition, UC-ZrC alloys are being considered for nuclear thermal propulsion systems given high melting temperatures such a system can have [6]. UC has good creep behavior up to 1273 K [3,4], and it can be used in synthesizing mixed carbides such as (U, Pu)C [7,8] or carbonitrides (U(C, N)) [9], which has superior resistance to hydrolysis [10], In the past, uranium carbide-beryllium system has also been considered as a nuclear reactor fuel-cladding material due to favorable properties of UC and Be that has a low neutron cross section [11]. The low neutron cross section of carbon also makes UC an easy to handle compound during post-irradiation chemical processing [3].

* Corresponding author at: Pacific Northwest National Laboratory, Richland, WA 99354, USA.
E-mail address: chinthaka.silva@pnnl.gov (C.M. Silva).

https://doi.org/10.1016/j.jnucmat.2024.155495
Received 15 July 2024; Received in revised form 3 October 2024; Accepted 1 November 2024
Available online 2 November 2024

Three types of uranium carbides have been reported in the literature based on experimental data. Among them, the monocarbide (UC) composition is the most common phase, while the dicarbide composition (UC_2) is also stable under ambient conditions. However, the third carbide, uranium sesquicarbide (U_2C_3), is only observed experimentally at high temperatures such as 2273 K [12,13], UC has a NaCl-type face centered cubic (*fcc*) structure with a space group of *Fm*-3 m [14]. Two polymorphs have been reported for the dicarbide system: α-UC_2 with the CaC_2-type body centered tetragonal with a space group of *I4/mmm* and β-UC_2 with the NaCl-type face centered cubic structures [14,15]. The β-UC_2 has only been reported to form at elevated temperatures (e.g., 2038 K) [16]. A range of lattice parameters has been reported for these carbide systems due to their ability to form stable non-stoichiometric compositions and the dissolution of impurities such as oxygen in their unit cells [17].

The most common technique that has been used in synthesizing UC in laboratory settings is the carbothermic reduction of UO_2 in which the oxide is reduced into UC using carbon under vacuum or inert atmospheric conditions. Literature shows that the carbothermic reduction of UO_2 can be performed at low temperatures (1573 – 1773 K) with incomplete reaction [13] as well as at high temperatures (1773 – 2273 K) with complete reaction. For composite carbides such as UC-ZrC, it requires very high temperatures such as 2623 – 2973 K [18].

The use of low temperatures is also important in mixed carbide synthesis such as (U, Pu)C in which significant levels of Pu can vaporize from the system during the synthesis, even at as low as 1823 K [7,19]. Even though the reaction mechanism is well understood for this reduction conversion of UO_2 into UC, it is scarce to find data regarding its reaction kinetics, which is one of the important data sets needed in further experimental evaluations such as enabling large-scale synthesis and computational/modeling investigations. Therefore, the low-temperature carbothermic reduction of UO_2 to UC was used in this work to study the UO_2 reduction kinetics at four different temperatures: 1623, 1673, 1748, and 1762±276 K. Two different sample holding crucibles (Al_2O_3 and graphite) were used to understand the non-stochiometric and oxygen dissolution behavior in the uranium monocarbide. Inert ($Ar_{(g)}$) and reducing (Ar-4%$H_{2(g)}$) atmospheres were used for the samples synthesized using Al_2O_3 crucible, while only inert ($Ar_{(g)}$) atmosphere was used for the samples synthesized using graphite crucible.

2. Experimental details

2.1. Precursor material

Depleted uranium dioxide (UO_2) was mixed with carbon (C) nano powder (<100 nm Sigma Aldrich) at 3.1:1 C/UO_2 molar ratio using a mortar and pestle in a glove box for 30 – 60 min. The C/UO_2 molar ratio of 3.1 was used based on the reaction (Eq. (1)) plus an extra 0.1 molar C to compensate for any loss of C during precursor preparation and sample handling. A 3.5 C/UO_2 molar ratio feedstock was also made for a few extra experiments. These two precursor compositions will be reported as UO_2–3.1C and UO_2–3.5C from herein. Either an Al_2O_3 or graphite crucible in their post-baked conditions was used to hold the UO_2/C samples, and a tube furnace (Thermo Scientific™, Lindberg/Blue M™ 1773 K General-Purpose Tube Furnace) was used for the heat treatments. This tube furnace could operate at a maximum temperature of ≤1773 K. A ramping rate of 285 – 296 K/min was used for all the experiments conducted at temperatures ≤1673 K, while 281 K/min rate was used for temperatures ≥1748 K. Furnace cooling was used for the cooling step.

$$UO_{2(s)} + 3\ C_{(s)} \rightarrow UC_{(s)} + 2\ CO_{(g)} \quad (1)$$

2.2. Carbothermic reduction

Literature indicates that the formation of UC starts at around 1773 K and UO_2 and C content start to decrease at around 1714 K during the carbothermic reduction of UO_2/C mixture [20]. In this experiment, carbothermic reduction was therefore conducted at ≤1773 K to study the reaction at relatively low temperatures. As will be discussed in the results and discussion sections, UO_2/C precursor samples were heat treated at different temperatures for varied dwell times under inert (argon) or reducing (Ar-4%H_2) flowing cover gas environments. $Ar_{(g)}$ (UHP or ultra-high purity grade) cover gas was swept through Cu powder heated at 773 K to getter O_2 before it was introduced to the tube furnace that undertook the carbothermic reduction of the samples.

2.3. Characterization

Powder X-ray diffraction (XRD) patterns of the samples were collected using a D8 Discover (Bruker Inc.) X-ray diffractometer Cu K_α radiation. A LaB_6–660c standard from National Institute of Standards and Technology (NIST) was used to correct the sample displacement error during Rietveld refinement using General Structure and Analysis System (GSAS) software [21].

Vacancy density of UC was estimated using $N_v = N \times e^{-\frac{Q_v}{K \times T}}$, where Nv, N, Qv, K, and T are number density of vacancies, total number of available lattice points, energy of vacancy formation, Boltzmann constant, and temperature, respectively [22].

3. Results

3.1. Carbothermic reduction of UO_2–3.1C in an alumina crucible

The first set of carbothermic reduction experiments was conducted in the Al_2O_3 crucible by varying reaction time (2 – 36 h) at 1673 K. Since the product phases were rich with oxygen in the form of oxides or oxycarbides when using Al_2O_3 crucible, these samples were used to discuss the non-stochiometric and oxygen dissolution behavior in the uranium monocarbide. A summary of the data of those samples is depicted in Table 1.

After a reaction time of 2 h at 1673 K, a partial conversion of UO_2–3.1C mixture into uranium carbide phase (31.5(1) wt.%) was observed under $Ar_{(g)}$ in UCA1 sample. In addition to the peaks corresponding to the reflections of the carbide and the unreacted UO_2 phases, two sets of broad peaks near UO_2 peaks and adjacent to carbide peaks but towards the high angle direction were also observed in this 2 h sample. These two sets of separate peaks echo the peaks corresponding to the Bragg reflections of oxide and carbide phases with smaller unit cells because they reside at higher angles than their parent phases. The

Table 1
XRD data of UC phase of the samples synthesized at 1673 K using an Al_2O_3 crucible. UCA1 has other phases (UO_2, $UC_{2-y}O_y$, $UC_{1-x}O_x$, 41.4(1), 20.8(6), 6.3 (1), respectively). UCA2 sample consists of $UC_{2-y}O_y$ and $UC_{1-x}O_x$ impurity peaks. UCA4 sample consists of $UC_{2-z}O_z$ impurity peaks. Full width at half maximum (FWHM) for (111) peak is also given.

Name	Time, h	Wt.%		Lattice parameter, nm		UC (111) peak	
		UC	σ	UC	σ	°2θ	FWHM
UO_2–3.1C, 1673 K, Ar							
UCA1	2	31.5	0.1	0.49621	0.00001	31.21	0.0399
UCA2	12	85.5	0.8	0.49563	0.00001	31.24	0.0531
UCA3	24	90.5	0.4	0.49385	0.00001	31.29	0.1957
UCA4	36	56.3	0.5	0.49244	0.00001	31.44	0.1246
UO_2–3.1C, 1673 K, Ar-4%H_2							
UCAH1	6	9.7	0.4	0.49428	0.00004	31.32	0.0798
UCAH2	12	52.4	0.5	0.49510	0.00001	31.27	0.0260
UCAH3	24	63.4	0.6	0.49231	0.00001	31.45	0.1116
UCAH4	36	63.3	0.6	0.49190	0.00001	31.50	0.1545

secondary carbide phase with the Bragg peaks adjacent to UC might have some oxygen dissolved in its lattice since it has a smaller unit cell. It is not uncommon to have some oxygen dissolved in UC as it is reported to have up to one-third of carbon atoms replaced by oxygen forming uranium oxycarbide as an intermediate phase of the carbothermic reduction of UO_2 [23,24]. Therefore, these peaks were fitted with a second carbide phase, which will be denoted using a general chemical composition of $UC_{1-x}O_x$ assuming stoichiometric compositions from herein.

The phase corresponds to the peaks next to UO_2 should have a crystal structure similar to that of UO_2 with a smaller unit cell than UO_2. There is also a carbide *fcc* phase β-UC_2 with NaCl-type structure (space group of *fm*-3 m) [15]. The lattice parameter of UC_2 (0.5488 nm) is also ~0.4% larger than that of UO_2 (0.54682 nm) [15,25]. Even though it is common practice to consider the size of atoms in a compound to in their form (ionic or covalent) in the compound, UO_2 is considered to have both ionic and covalent bonding characteristics. Ionic radius of O^{-2} is larger than that of C^{+4}, while covalent radius of oxygen is smaller than that of carbon [26,27]. Therefore, the second phase with Bragg peaks next to UO_2 phase will be regarded as a dicarbide dominant UO_2 and UC_2 mixed phase with a hypothesized chemical composition of $UC_{2-y}O_y$ henceforth. Such composition is also feasible as UC_2 usually represents a chemical composition in a range of $UC_{1.75}$ – $UC_{1.8}$ and that it is also considered as a $UC_{2-y}O_y$ phase due to the stabilizing nature of oxygen in the dicarbide structure [4,28]. The successfully carried out full profile fit of the 2 h sample's XRD pattern using these phases is shown in Fig. 1a with highlighted separate phases in Fig. 1b. The refined LPs of UC, $UC_{1-x}O_x$, UO_2, and $UC_{2-y}O_y$ are 0.49621(1), 0.49017(1), 0.54704(1), and 0.53294 (1) nm, respectively. The high end lattice parameter of 0.49621(1) obtained for UC indicates a hyperstoichiometric uranium monocarbide as was reported in the literature such as 0.49610 ± 0.00004 nm for a composition of $UN_{1.006}$ [29]. The lower LPs of the secondary phases with Bragg reflections next to UC and UO_2 main phases also verify the presence of these secondary phases with the hypothesized compositions of $UC_{1-x}O_x$ and $UC_{2-y}O_y$, respectively, as was observed in an earlier study [30].

When the reaction time was increased from 2 h to 12 h (UCA2 sample), most of the UO_2–3.1C mixture converted into the carbide phase, while the conversion was highest for the 24 h UCA3 sample. As in the 2 h sample, the 12 h sample also showed some minor peaks for the $UC_{2-y}O_y$ and $UC_{1-x}O_x$ phases as depicted in Fig. 2. Because of the presence of broader carbide phase peaks in the 12 h sample than that of the 2 h sample (peak widths of (111) reflection is shown in Table 1), the separation of the peaks corresponding to the two carbide phases are narrower in the 12 h sample. This indicates a higher carbide and oxycarbide solid-solution (UC–$UC_{1-x}O_x$) behavior in that sample. In the 24 h sample, only the monocarbide and UO_2 phases were identified. The peak intensities for the first two main reflections of UO_2 (111 and 200) in this sample were also minor, while some considerable peak intensity was observed in the peaks in 45 – 70° 2Theta region. Therefore, UO_2 was also fitted during the Rietveld analysis of the 24 h sample's XRD pattern resulting in ~10 wt.% UO_2 in the sample. The peak broadening of the monocarbide phase is highest in the 24 h sample, indicating a direct proportionality between peak broadening and reaction time of the carbothermic reduction. The peak broadening of the 24 h sample also spans a 2Theta region covering the peak positions of the main monocarbide phase and the secondary oxycarbide phase ($UC_{1-x}O_x$), which was present in the 2 and 12 h samples (Fig. 2). An increase in the shift of the carbide peaks to higher angles with the reaction time as depicted by (111) carbide peak in Fig. 2 can also be observed. This peaks shift corresponds

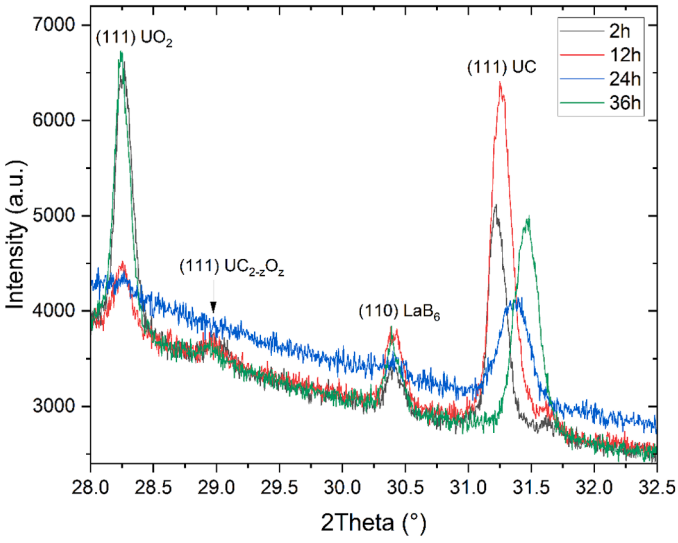

Fig. 2. Comparison of XRD patterns of samples (UCA2, UCA3, and UCA4) synthesized at 1673 K under $Ar_{(g)}$ using UO_2–3.1C precursors in Al_2O_3 crucible. Only 28 – 32.5° region out of 10 – 120° 2Theta is shown for clarity.

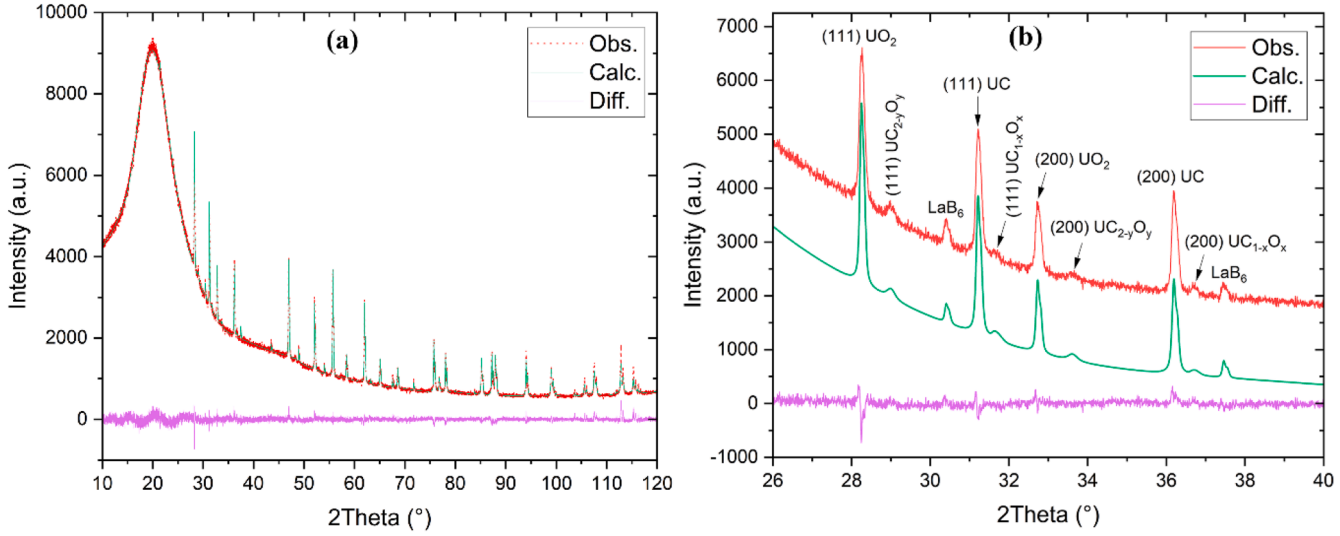

Fig. 1. XRD pattern of the UCA1 sample synthesized using UO_2–3.1C in an Al_2O_3 crucible at 1673 K under Ar for 2 h showing (a) full profile fit using Rietveld refinement and (b) an enlarged area (inset) showing separate peak positions of the 5 phases used in the refinement. Note that the calculated pattern in (b) is plotted with an offset to show the separate patterns clearly. Red, green, and pink colors represent the experimental, calculated, and difference plots, respectively.

to a decrease in the LP of the carbide as a function of the reaction time as can be observed in Table 1.

The increase in monocarbide phase content, decrease in the content of the secondary oxygen-dissolved phases, and the decrease in lattice parameter together with increasing peak width of the monocarbide phase of the samples held in Al_2O_3 crucibles with the increase in the reaction time indicate that oxygen dissolution increases in the main carbide lattice forming another $UC_{1-x'}O_{x'}$ type phase. This $UC_{1-x'}O_{x'}$ will be therefore an average composition of UC and the secondary $UC_{1-x}O_x$, with a larger unit cell size in $UC_{1-x}O_x$ than $UC_{1-x'}O_{x'}$ and $x'>x$.

A significant oxide phase content (43.7(5) wt.%) was observed in the 36 h sample (UCA4). Since the UO_2–3.1C conversion reaction into the carbide was close to a completion after the 24 h reaction time (UCA3 sample), the presence of close to 50 wt.% UO_2 in the 36 h sample indicates that the carbide was reoxidized into UO_2. The oxide formation could be due to a couple of reasons: the sample's exposure to impurity oxygen in the cover gas over a prolonged time or oxygen leaching from the tube furnace parts and the Al_2O_3 crucible used. The monocarbide peak shift to higher angles and the corresponding lowest lattice parameter among the samples also show that the highest level of oxygen dissolution is in this 36 h sample. Also, these lattice parameters are $<0.4948\pm0.001$ nm, which is reported as the lattice parameter for maximum solubility of oxygen in UC corresponding to 35 mole% UO ($UC_{0.65}O_{0.35}$) for a 1373–2573 K temperature range [31], observed in the samples could be attributed to a non-equilibrium state of the carbide phase under prolong (24 and 36 h) heat treatment in a high oxygen partial pressure environment.

Another sample (UCAH3) was synthesized using the same precursor in an Al_2O_3 crucible and at same temperature with a reaction time of 24 h under a reducing environment (Ar-4%H_2) aiming to lower the possible oxidation reaction of the carbide or the dissolution of oxygen in the carbide lattice. However, that sample also contained 36.6(6) wt.% UO_2 and the rest being uranium carbide. Since the lattice parameter (~0.494 nm) of the sample is also lower than all other samples synthesized under $Ar_{(g)}$ in Al_2O_3 crucible and that it has a significant amount of UO_2, it may indicate that the oxide to carbide conversion occurs faster under reducing conditions than under inert atmospheric conditions or some C is removed as $CH_{4(g)}$ and other short chain hydrocarbons resulting less C in the precursor for the oxide to convert to carbide. In order to test these hypotheses, three more samples were synthesized under Ar-4%H_2 by varying the reaction time at 1673 K. As depicted in Table 1, only ~10 wt.% UC formed after a 6 h reaction time in UCAH1 sample, while it increased to 52 wt.% by increasing the reaction time to 12 h in UCAH2 sample. The amount of UC in the product after 36 h (UCAH4) reaction time was similar to that of the 24 h reaction time. If UC oxidation or dissolution of oxygen at small scale occurs under these experimental conditions, the amount of UO_2 should be greater in the 36 h reaction time sample. Since it is not the case, the second hypothesis of removal of C from the precursor can be identified as the main cause for the incomplete conversion of UO_2 into UC under Ar-4%H_2. It is also observed that the refined lattice parameter of the product monocarbide in the 12 to 36 h samples also decreased from 0.4951 to 0.4919 nm as the reaction time increased under Ar-4%H_2. This observation suggests that more U to dissolve in the carbide resulting hypostoichiometric UC_{1-a} [32] due to the lack of C in the reaction medium under prolong heating under the reducing conditions. This observation is also in agreement with the reported observation of dissolution of U in UC lattice forming C vacancies and thereby forming a hypostoichiometric composition when the reaction medium temperature is increased [33]. Furthermore, the significantly low lattice parameters (~0.492 nm) in samples with reaction times of 24 and 36 h and the increase in peak widths with the decrease in the lattice parameters of these 4 samples also suggest the dissolution of oxygen in the UC lattice of those samples due to the already existing oxygen from the unreacted UO_2 and the non-stoichiometric UC_{1-a} due to incomplete reaction. It should also be noted that vacancies usually form defect structure and results lattice expansion. In this case, however, the lattice parameter decreased, suggesting higher effect of the presence of free U, which has been reported to be observed in the grain boundaries of the carbide [22,34], than the defect structure. Thus, it can be concluded that the decrease in the lattice parameters of the monocarbide phase in these samples are due to both the dissolution of oxygen in UC lattice, as the LP of uranium monoxide is smaller (0.492(2) nm) [12,35], and non-stoichiometric UC_{1-a} formation due to incomplete reaction.

3.2. Carbothermic reduction of UO_2/C mixtures in a graphite container

As discussed in Section 3.1, single-phase UC was not obtained and the XRD data indicates the presence of dissolved oxygen in the carbide lattice synthesized using the carbothermic reduction of UO_2–3.1C at 1673 K using an alumina crucible. Therefore, a few more experimental conditions were evaluated using a graphite crucible to hold the samples, reducing the oxygen partial pressure in the furnace reaction chamber. These experimental conditions included a few different synthesis temperatures, two different precursor compositions, and reaction times varying from 2 to 24 h (Table 2).

In a graphite crucible at 1623 K and with UO_2–3.1C precursor, UC formation was observed but only at <5 wt.% after a reaction time of 6 h in UCC1 sample. The UC content increased to 15 wt.% in the second sample (UCC2) held for 12 h at 1623 K. Increasing the reaction time to 20 h only increased the UC fraction to 18 wt.% in UCC3 sample further indicating slow reaction progress at 1623 K. Lattice parameters of these three samples synthesized at 1623 K are 0.4936 – 0.4938 nm with a minor increase (0.03 – 0.04%) in 12 and 20 h samples with respect to the 6 h sample.

Close to 50% oxide to carbide conversion was observed in UCC4 sample after 4 h reaction time at 1673 K using UO_2–3.1C precursor with unreacted UO_2 as the only second phase (Fig. 3a). The conversion reaction reached ~75 and ~100% completion with 10 (UCC5) and 18 h (UCC6) reaction times at 1673 K, respectively, while only minor peaks (asterisk marks in Fig. 3a) were present for the UO_2 phase leading to <5 wt.% in the later (18 h) sample. While all three 1673 K samples had larger lattice parameters than that of 1623 K samples, a 0.06% decrease in LP was observed in the 18 h sample compared to 0.01% increase in 10 h sample with respect to 4 h sample.

In a graphite crucible at 1748 K, the carbothermic reduction of UO_2–3.1C was ~20% complete after 2 h reaction time in UCC7 sample.

Table 2
XRD data of UC phase of the samples synthesized using a graphite crucible. UCC13 sample has amorphous broad background at UO_2 peak positions. UCC14 has amorphous hump at UO_2 peak positions. UCC10 has a slight hump at ~29° 2Theta. Note that all these samples consisted of either only UC or UC and UO_2 phases.

Name	Time, h	UC wt.%	σ	UC LP, nm	σ	LP increase,%
UO_2–3.1C, 1623 K, Ar						
UCC1	6	3.8	0.3	0.49361	0.00001	N/A
UCC2	12	14.8	0.3	0.49376	0.00001	0.03
UCC3	20	18.0	0.4	0.49382	0.00001	0.04
UO_2–3.1C, 1673 K, Ar						
UCC4	4	43.5	0.5	0.49593	0.00001	N/A
UCC5	10	73.5	0.5	0.49596	0.00001	0.01
UCC6	18	94.3	0.4	0.49565	0.00001	−0.06
UO_2–3.1C, 1748 K, Ar						
UCC7	2	19.2	0.4	0.49555	0.00001	N/A
UCC8	4	70.3	0.5	0.49598	0.00001	0.09
UCC9	6	100.0		0.49605	0.00001	0.10
UO_2–3.1C, 1762±276 K, Ar						
UCC10	2	43.5	0.5	0.49562	0.00001	N/A
UCC11	4	51.5	0.5	0.49590	0.00001	0.06
UCC12	6	97.1	0.8	0.49593	0.00001	0.06
UO_2–3.5C, 1673 K, Ar						
UCC13	12	85.4	0.6	0.49569	0.00001	N/A
UCC14	24	~100		0.49549	0.00001	−0.04

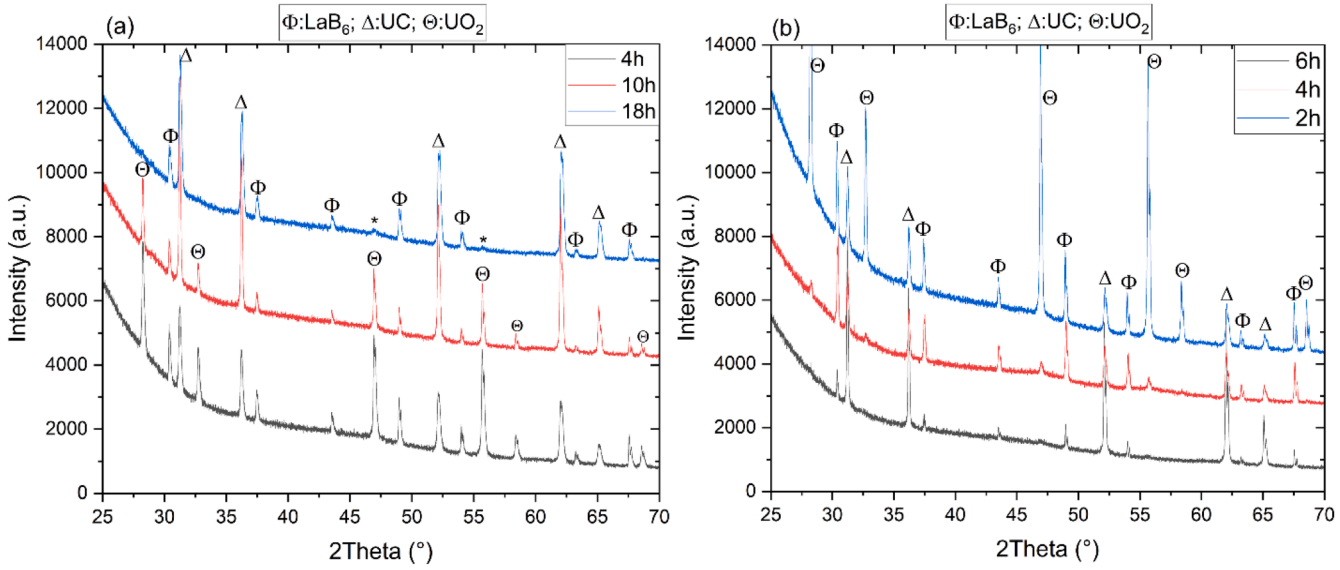

Fig. 3. XRD patterns of UC samples synthesized at (a) 1673 K and (b) 1748 K using UO_2–3.1C precursors in graphite crucible. Asterisks highlight minor UO_2 peaks in the 18 h sample.

A greater conversion of oxide to carbide was observed when the reaction time increased to 4 h in UCC8 sample with a 70% conversion and a 100% conversion after 6 h in UCC9 sample (Fig. 3b). The refined lattice parameter of the carbide phase also increased with the increase in its formation with 0.09 and 0.1% increase in the 4 h and 6 h samples compared to the 2 h sample, respectively. The change in lattice parameters of samples synthesized at 1673 and 1748 K is only ~0.5%, while it was not significant for 1623 K samples. The lowest level of formation and the smallest lattice parameters of the monocarbide phase of the samples synthesized at 1623 K with reaction times up to 20 h suggest that the carbide phase is in a non-equilibrium state.

To compare the product phase characteristics, another three samples were synthesized with a target temperature of 1773 K. However, due to the difficulties of achieving the targeted temperature in the used tube furnace, the maximum temperature that could be achieved was a 1759 – 1765 K temperature range (1762±276 K). As depicted in Table 2, a greater fraction of UC was acquired at 1762±276 K than that at 1748 K with similar 2 h reaction time in UCC10 sample as expected. Two other samples made using 4 h (UCC11) and 6 h (UCC12) reaction times at 1762±276 K also showed a similar trend in UC formation compared to 4 and 6 h samples at 1748 K. The lattice parameters of UC phase also showed an increasing trend with respect to the level of reaction completion. The lattice parameters of 1673, 1748, and 1762±276 K samples were also comparable with the reported values of stoichiometric UC. 12.[36]

Since the carbothermic reduction reaction was complete after 18 h processing time at 1673 K for the UO_2–3.1C sample, two more samples were synthesized using a slightly greater carbon content (C/UO_2 molar ratio of 3.5) in the precursor at 1673 K with 12 to 24 h reaction times to evaluate the effect of precursor C level on the product phases. Similar reaction kinetics were observed for both UO_2–3.1C and UO_2–3.5C precursors at 1673 K (Table 2). The UCC13 sample synthesized using a 24 h reaction time only showed amorphous humps at peak positions of UO_2 phase in the XRD pattern compared to the minor developed peaks observed in the 12 h UCC14 sample, suggesting insignificant effect on the product phases of the samples after 18 h reaction time at that temperature.

3.3. Kinetics of carbothermic reduction of UO_2–3.1C in a graphite container

During the carbothermic reduction, the evolution of only a slight amount of $CO_{2(g)}$ was reported [7], while the formation of UC involves the evolution of gaseous carbon monoxide ($CO_{(g)}$) as depicted by Eq. (1). This would imply a rate determining step of diffusion of gaseous species out of the solid crystals involved in the reaction. However, evolution of gases is generally faster than a diffusion reaction involving a solid-solid reaction. Therefore, formation of UC via the diffusion reaction of C with UO_2 is assumed to be the rate limiting step for the determination of reaction kinetics discussed below.

The rate of the carbothermic reduction of UO_2 depends on the concentration of the reactant UO_2 at a given time. As discussed earlier (Table 2), only UC(s) or UC(s) and unreacted UO_2(s) phases were observed in the terminal products synthesized using carbothermic reduction of UO_2–3.1C in graphite crucible. Because of this reason, the change in the concentration of reactant (UO_2) was inversely proportional to the change in the formation of product (UC) in each sample for all temperatures tested. This observation suggests that the rate of the carbothermic reduction of UO_2 via C diffusion into UO_2 forming UC can be written using the concentration of product UC.

Jander et al. [37] and Namba et al. [38] have reported two rate equations depicted by Eq. (2) and Eq. (3), respectively for similar solid-state reactions that occur via the diffusion reaction mechanism. Out of these two rate equations, Eq. (3) has been used in a similar system (i.e., ThO_2+UO_2+C) Namba et al. and also resulted in the best fit for our data. Therefore, the experimental data were plotted with respect to $\left(1-\sqrt[3]{(1-X)}\right)^2$ vs t according to Eq. (3) as shown in Fig. 4a. The rate constants for each temperature used here were then determined using the slope of unweighted linear fits of the data and are shown in Table 3.

$$\left(1-\sqrt[3]{\frac{100-X}{100}}\right)^2 = k't \tag{2}$$

$$\left(1-\sqrt[3]{(1-X)}\right)^2 = k't \tag{3}$$

Where X is the concentration of the UC in wt.% formed at a given time t.

The rate constants of the reaction at each temperature were also used in plotting the data according to the Arrhenius equation (Eq. (6)). A

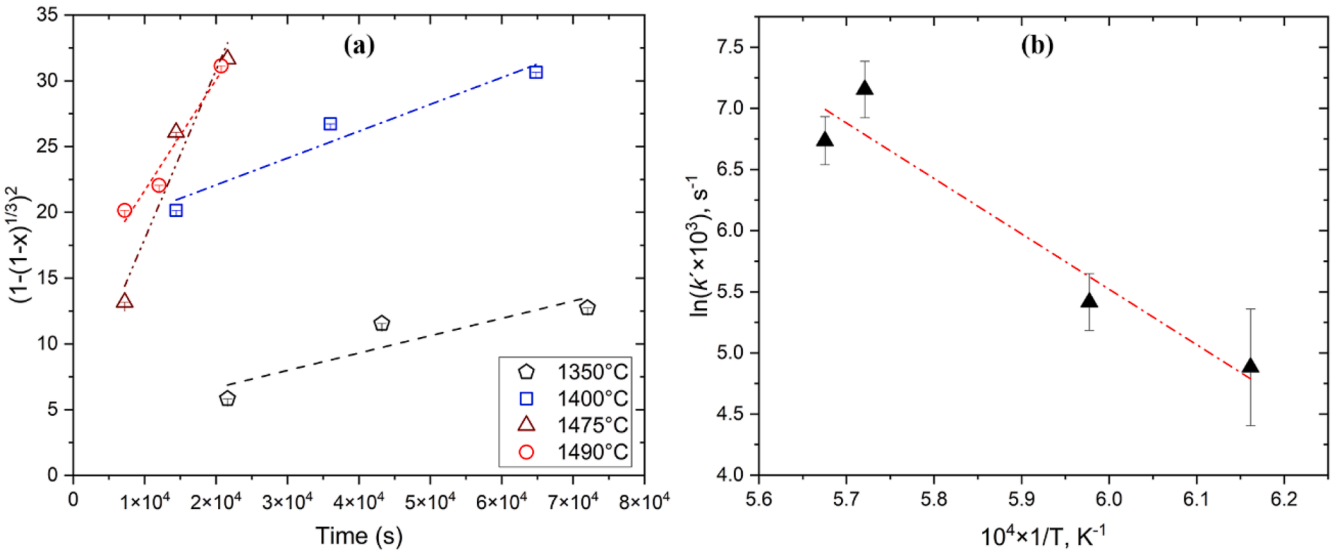

Fig. 4. Reaction kinetics of carbothermic reduction of UO_2–3.1C. (a) Change in UC concentration against time at four different temperatures and (b) Arrhenius plot of rate constants against temperature. Dashed lines show unweighted linear fits of the data.

Table 3
Reaction rate constants at four different temperatures.

Temperature (K)	Rate constant	
	k' ($10^{-3} \times s^{-1}$)	Error, $\sigma_{k'}$
1623	0.132	0.063
1673	0.204	0.047
1748	1.280	0.295
1762±276	0.841	0.166

slope of −4.533±0.902 in the Arrhenius plot (Fig. 4b) resulted in an activation energy of 377±75 kJmol^{-1} for the carbothermic reduction of UO_2–3.1C in a graphite crucible up to a maximum reaction temperature of 1762±276 K. This activation energy will be compared with the reported values in the discussion section (Section 4).

$$\ln k' = -\left(\frac{E_a}{R}\right)\left(\frac{1}{T}\right) + \ln A \quad (6)$$

Where E_a, R, and A are activation energy, ideal gas constant (8.314 J K^{-1} mol^{-1}), and pre-exponential factor, respectively.

4. Discussion

A range of LPs (0.4951 – 0.4965 nm) is reported in the literature [12, 39–41], while a lattice parameter value of 0.49605(4) nm was reported for stoichiometric uranium monocarbide UC by Williams et al. [36]. That publication also have reported two ranges of LPs: 0.49600(5) – 0.49550(3) nm for $a = 0.00 – 0.10$ and 0.49520(2) – 0.49562(7) nm for $b = 0.21 – 0.51$ for a composition of $UC_{1-a\ (and\ b)}$ in as-synthesized samples [42]. For annealed samples at 1573 K for up to 88 h, they reported 0.49601(2) – 0.49570(3) nm lattice parameter range for $b = 0.00 – 0.51$. They also indicated that this change in lattice parameter is because of the change in carbon content and not due to oxygen or nitrogen contamination in the uranium monocarbide lattice. This information is depicted in Fig. 5 together with the change in lattice parameter against the UC wt.% of the samples synthesized using Al_2O_3 (Table 1) and graphite (Table 2) crucibles in this study.

In an Al_2O_3 crucible the carbothermic reduction of UO_2 and 3.1 molar C mixture under flowing Ar cover gas produced a carbide phase

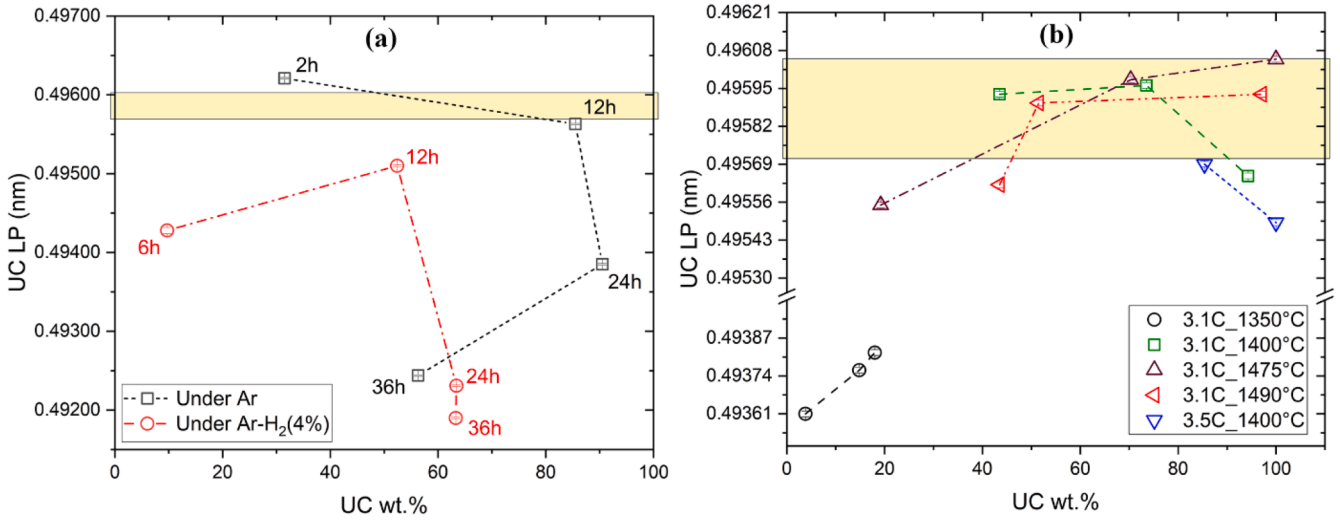

Fig. 5. Variation of lattice parameters of UC against its wt.% in the samples synthesized using (a) Al_2O_3 and (b) graphite crucibles. The lattice parameter range of 0.49570 – 0.49605 nm for $x = 0.34 – 0.50$ mol for a composition of $U_{1-d}C_d$ from Williams et al. [36,42] is highlighted in the figure.

up to 90 wt.% phase purity at 1673 K using 12 – 24 h reaction times. However, an increase in the reaction time decreased the UC lattice parameters, which are lower than the reported values for UC_{1-a} as depicted in Fig. 5a and discussed above. This suggests that the decrease in the lattice parameter of the monocarbide phase in these samples synthesized using Al_2O_3 crucible is due to the dissolution of oxygen forming uranium monoxycarbide ($UC_{1-x}O_x$) phase as is reported not only in UC but also in mixed carbides such as (U, Pu)C [43], Its lattice parameter significantly decreased at 36 h reaction time and decreased the carbide phase fraction in the product due to reoxidation of the carbide phase and oxygen dissolution in the remaining UC lattice. The dissolution of oxygen in UC is not unusual as it has a NaCl-type structure containing 8 non-metal octahedral interstices that permit the dissolution of impurity elements. When a reducing (Ar-4%H_2) environment was used for the carbothermic reduction of the precursor in an Al_2O_3 crucible, only up to 63 wt.% of monocarbide phase formed even up to 36 h reaction time with a decrease of the carbide unit cell size. These observations suggest incomplete reaction due to loss of C under reducing conditions and the dissolution of oxygen from the precursor in the carbide phase.

When graphite crucibles were used to hold the UO_2–3.1C precursors, only UC and unreacted UO_2 were observed in the products. At 1623 K up to 20 h reaction time, low lattice parameters (Fig. 5b) were obtained for the monocarbide phase, suggesting UC in a non-equilibrium state. The refined LPs (0.49590(1) – 0.49605(1) nm) of the samples synthesized in this current study using UO_2–3.1C precursors at 1673 – 1762±276 K with holding times of 2 – 10 h, even in partially converted carbide products in graphite crucibles, indicate that these samples have chemical compositions close to stoichiometric UC as compared to the reported data (Fig. 5b). The sample synthesized with a holding time of 18 h at 1673 K however has a smaller lattice parameter (0.49565(1) nm and a 0.08% decrease compared to 0.49605(1) nm), which matches the Williams's reported lattice parameters of two different carbide compositions: $U_{0.67}C_{0.33}$ and $U_{0.51}C_{0.49}$ [42]. A recent study also reported a lattice parameter of 0.49562 nm for a composition of $U_{0.51}C_{0.49}$ (or $UC_{0.97}$) and for oxygen-dissolved carbide with the composition of $UC_{0.97}O_{0.03}$ [44]. Therefore, a nominal composition close to $U_{0.51}C_{0.49}$ can be inferred to this carbide synthesized here assuming the dissolved oxygen level in the carbide lattice is insignificant.

Similarly, the refined lattice parameter of the sample synthesized using UO_2–3.5C precursor at 1673 K with a holding time of 24 h was smaller (a 0.04% decrease) than that of the 12 h sample, while the later matching a nominal composition of $U_{0.51}C_{0.49}$ and the former resulting a composition of $U_{1-d}C_d$ with 'd' equal to 0.37 or 0.47. A slightly smaller lattice parameter was also observed in the sample synthesized at 1673 K with a reaction time of 18 h for UO_2–3.1C precursor. These two observations suggest that uranium monocarbide starts to deviate from its stoichiometric composition of UC when the reaction time (or synthesis holding time) is >10 h at the tested temperature of 1673 K regardless of the precursor C/UO_2 molar ratio, suggesting more than 0.1 molar extra carbon is not needed to complete the carbothermic reduction of UO_2 represented by Eq. (1).

The U–U bond length increases with the increase of lattice parameter of UC as depicted in Fig. 6a. The U–C bond length also increases with the increase in its lattice parameter, but it plateaued out at a maximum value of 0.248 nm and a nominal lattice parameter of 0.496 nm, which relates to near stoichiometric UC. As shown in Fig. 6b, C vacancy density of UC also increases with temperature. A vacancy density range of 0.67 × 10^{20} – 1.10 × 10^{20} cm^{-3} was determined for the UC synthesis temperatures (1623 – 1765 K) tested in this study. It is reported that there is a slight distortion in the carbide unit cell resulted from the uranium nearest neighbors surrounding the C vacancy in UC_{1-a} moving toward the vacancy [44]. This also results in a lower U-C bond length compared to that of the near stoichiometric UC unit cell. As the lattice parameter increases and approaches that near stoichiometric composition, the density of C vacancies at a particular temperature also starts to decrease making the U-C bond to rearrange to its near stoichiometric value and lowering the distortions. Once the near stoichiometric UC composition is reached, U-C bond lengths max out plateauing out as observed in Fig. 6a. On the other hand, U-U distance keep increasing to compensate the unit cell growth. This change in U–C bond length with respect to the change in lattice parameters further confirms the presence of vacancies and substochiometric behavior of uranium monocarbide phase in the samples synthesized here. However, this data (behavior of U–C bond length against lattice parameter) cannot be used to verify the presence of oxygen interstitials in the uranium monocarbide unit cells with lattice parameters <0.49520(2) nm, which is reported as the lowest end for the UC_{1-a} hypostoichiometry [42].

Since only UC and unreacted UO_2 were present in the products of the samples synthesized using the carbothermic reduction of UO_2+C mixture under inert atmosphere ($Ar_{(g)}$ cover gas and graphite crucible), the diffusion reaction between UO_2 and C to form UC could be used to determine activation energy of the reaction. The Pseudo first-order rate equation reported for ThO_2+UO_2+C system best fitted the data that were acquired in this study, and therefore used to determine the activation energy of the reaction at the relatively low reaction temperatures tested here [38]. The activation energy reported for the carbothermic reduction of ThO_2+UO_2+C mixture was 320 kJ mol^{-1}, which is within the range (302 – 452 $kJmol^{-1}$) we report for UO_2–3.1C mixture (377±75 $kJmol^{-1}$). Another study also reported activation energies of 209±84 $kJmol^{-1}$ and 268±84 $kJmol^{-1}$ for the diffusion of C and U in UC [45].

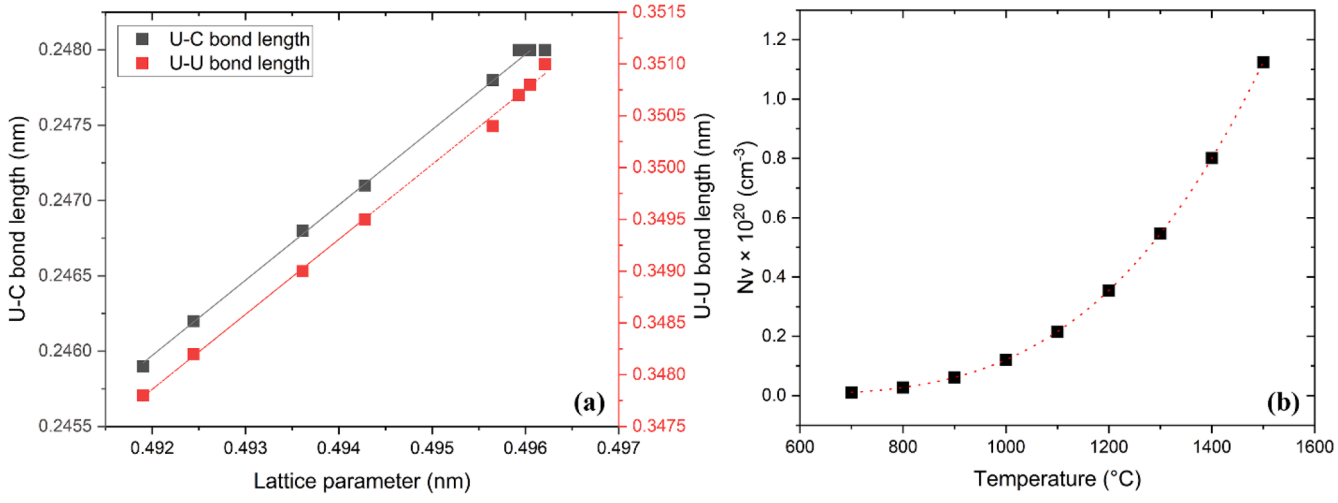

Fig. 6. (a) U-U and U-C bond lengths of selected samples as a function of lattice parameter and (b) vacancy density of UC as a function of temperature.

Using the levels of evolved CO gas during the carbothermic reduction of porous UO_3+C microspheres, another study reported activation energies of 335±8.6 and 363.7 ± 7.6 kJmol^{-1} under reducing and flowing inert gas, respectively [46]. These activation energies are lower than that of the carbothermic reduction of UO_2, suggesting that diffusion reactions of C and U into UC and reduction in the form of porous microspheres are more energetically favorable than the diffusion reaction of UO_2 and C making UC in the powder form. Furthermore, the activation energy that is reported here is comparable with what was reported (375±20 kJ/mol^{-1}) for (U, Pu)C [47].

5. Conclusions

Carbothermic reduction of UO_2+C mixtures under inert and reducing conditions was tested here. Under flowing $Ar_{(g)}$ but with a considerably high oxygen partial pressure due to the used furnace chamber and Al_2O_3 crucible, the product consisted of UC, $UC_{1-x}O_x$, $UC_{2-y}O_y$, and UO_2 phases. The UC phase consisted of lower lattice parameters compared to what is reported in the literature, attributing to the dissolution of oxygen in UC lattice of these samples. Under reducing Ar-4%$H_{2(g)}$ environment, only up to ~65 wt.% of UC formation was observed, while smaller UC unit cell sizes were obtained for those samples. Since the reducing environment should remove the oxygen impurities and lower oxygen partial pressure in the experimental setup, the small UC unit cell sizes were attributed to a number of reasons including the incomplete reaction due to the loss of C from the reaction medium, the presence of oxygen in the reaction medium from the unreacted precursor UO_2, and the non-equilibrium state of product UC.

The samples synthesized using flowing $Ar_{(g)}$ inert environment with the use of graphite crucible to hold the samples produced the expected UC and only unreacted UO_2 when conditions for complete reaction were not satisfied. However, reaction temperatures of ≥1673 K and sufficient reaction time produced UC with lattice parameters comparable to the values reported for near stoichiometric UC. At 1623 K, UC formation was very low (up to 18 wt.%) even with a prolong reaction time (20 h), and the UC phase lattice parameters were also low, suggesting the incomplete reaction and the UC phase to be in a non-equilibrium state. At 1673 K, the use of 3.1 and 3.5 molar C to UO_2 in the precursors did not show significant difference in the product phases, indicating 3.1 molar C is sufficient for the carbothermic reduction of UO_2. The changes in U–C bonding also showed the presence of slight lattice deformation attributed to the U moving towards C vacancy sites and is related to the decrease in the lattice parameter of non-stoichiometric UC. A 377±75 kJmol^{-1} activation energy was also determined for the carbothermic reduction of UO_2+C mixture under inert atmospheres at ≤1773 K. This value is within the ranges of activation energies reported for the carbothermic reduction of similar systems.

The data presented here should support the understanding and controlling the purity of UC during its fabrication from carbon and UO_2 precursors. The use of low temperature carbothermic reduction of UO_2 is important as it will allow for efficient and low-cost UC nuclear fuel fabrication at industrial scale. Transmutation efforts of long-lived isotopes (e.g., ^{239}Pu and ^{241}Am), which come from the nuclear fuel cycle, in the form of next generation mixed carbide nuclear fuel can also benefit from the low temperature fuel fabrication conditions. Furthermore, the data including activation energy present in this study will be useful for modeling efforts to be carried out to learn more about the carbothermic reduction process parameters and the monocarbide system that is considered to be an alternate fuel for the conventional UO_2.

CRediT authorship contribution statement

Chinthaka M. Silva: Writing – original draft, Visualization, Validation, Resources, Methodology, Investigation, Formal analysis, Data curation, Conceptualization. **Kyle J. Kondrat:** Writing – review & editing, Validation, Resources, Methodology, Conceptualization. **Bradley C. Childs:** Writing – review & editing, Validation, Resources, Methodology. **Maryline G. Ferrier:** Writing – review & editing, Validation, Resources, Methodology. **Michelle M. Greenough:** Data curation, Writing – review & editing. **Kiel S. Holliday:** Conceptualization, Funding acquisition, Investigation, Project administration, Resources, Supervision, Validation, Writing – review & editing. **Scott J. McCormack:** Conceptualization, Funding acquisition, Investigation, Methodology, Resources, Supervision, Validation, Writing – review & editing.

Declaration of competing interest

The authors declare that they have no known competing financial interests or personal relationships that could have appeared to influence the work reported in this paper.

Acknowledgements

This research was performed under the auspices of the U.S. Department of Energy (DOE) by Lawrence Livermore National Laboratory (LLNL) under Contract No. DE-AC52-07NA27344. Authors also acknowledge support from the National Science Foundation (NSF), Division of Materials Research (DMR), Ceramic (CER) program under grant DMR 2047084.

Supplementary materials

Supplementary material associated with this article can be found, in the online version, at doi:10.1016/j.jnucmat.2024.155495.

Data availability

Data in the supplementary information.

References

[1] R.W. Jones, J.L. Crosthwaite, Uranium Carbide Fuel for Organic Cooled Reactors, Atomic Energy of Canada Limited, 1973. Report # AECL-4443.
[2] S. Legend, C. Bouyer, V. Dauvois, F. Casanova, D. lebeau, C. Lamouroux, Uranium carbide dissolution in nitric acid: speciation of organic compounds, J. Radioanal. Nucl. Chem. 302 (2014) 27–39.
[3] M. Brykala, M. Rogowski, Preparation of microspheres of carbon black dispersion in uranyl-ascorbate gels as precursors for uranium carbide, Prog. Nucl. Energy 89 (2016) 132–139.
[4] B.R.T. Frost, The carbides of uranium, J. Nucl. Mater. 10 (1963) 265–300.
[5] M.W. Mallett, A.F. Gerds, H.R. Nelson, The uranium-carbon system, J. Electrochem. Soc. 99 (1952) 197–204.
[6] D.P. Butt, T.C. Wallace Sr., The U-Zr-C ternary phase diagram above 2473 K, J. Am. Ceram. Soc. 76 (1993) 1409–1419.
[7] Y. Suzuki, T. Sasayama, Y. Arai, H. Watanabe, Fabrication of uranium-plutonium mixed carbide pellets, J. Nucl. Sci. Technol. 18 (1) (1981) 61–70.
[8] S. Rosen, M.V. Nevitt, A.W. Michell, The uranium monocarbide-plutonium monocarbide system, J. Nucl. Mater. 9 (1963) 137–142.
[9] C.M. Silva, T.B. Lindemer, S.R. Voit, R.D. Hunt, T.M. Besmann, K.A. Terrani, L. L. Snead, Characteristics of uranium carbonitride microparticles synthesized using different reaction conditions, J. Nucl. Mater. 454 (2014) 405–412.
[10] S. Sugihara, S. Imoto, Hydrolysis of uranium carbonitrides, J. Nucl. Sci. Technol. 7 (2) (1970) 67–71.
[11] J.F. Murdock, Reaction between beryllium and uranium monocarbide, J. Nucl. Mater. 7 (1962) 192–196.
[12] R.E. Rundle, N.C. Baenziger, A.S. Wilson, R.A. McDonald, The structures of the carbides, nitrides, and oxides of uranium, J. Am. Chem. Soc. 70 (1948) 99–105.
[13] H.M. Reiche, S.C. Vogel, M. Tang, *In situ* synthesis and characterization of uranium carbide using high temperature neutron diffraction, J. Nucl. Mater. 471 (2016) 308–316.
[14] A.E. Austin, Carbon positions in uranium carbides, Acta Crystallogr. 12 (1959) 159–161.
[15] A.L. Bowman, G.P. Arnold, W.G. Witteman, T.C. Wallace, N.G. Nereson, The crystal structure of UC_2, Acta Crystallogr. 21 (1966) 670–671.
[16] S. Chowdhury, D. Manara, O. Dieste-Blanco, D. Robba, A.P. Gonçalves, Laser heating study of the high-temperature interactions in nanograined uranium carbides, Materials 14 (2021) 5568.
[17] H. Tagawa, K. Fujii, Y. Sasaki, Studies on the uranium dicarbide phase, J. Nucl. Sci. Technol. 8 (5) (1971) 244–249.

[18] K. Davidson, W. Martin, D. Schnell, J. Taub, J. Taylor, Development of carbide-carbon composite fuel elements for rover reactors, los alamos scient. Laboratory Report LA-5005, 1972.
[19] P.E. Potter, The volatility of plutonium carbides, J. Nucl. Mater. 12 (1964) 345–348.
[20] H.M. Reiche, S.C. Vogel, M. Tang, In situ synthesis and characterization of uranium carbide using high temperature neutron diffraction, J. Nucl. Mater. 471 (2016) 308–316.
[21] Larson, A.C., Von Dreele, R.B. General structure analysis system (GSAS), Los Alamos National Laboratory Report LAUR 86-748 (2000).
[22] N.M. Killey, The secondary creep behavior of uranium monocarbide in compression. I: hypostoichiometric uranium monocarbide, J. Nucl. Mater. 41 (1971) 178–186.
[23] Carbides in nuclear energy, Nature 201 (1964) 27–30.
[24] W. Chubb, Carbides in nuclear energy, Nucl. Sci. Eng. 22 (1965) 500–501.
[25] S.A. Barret, A.J. Jacobson, B.C. Tofield, B.E.F. Fender, The preparation and structure of barium uranium oxide Ba UO3+x, Acta Cryst. 38 (1982) 2775.
[26] R.D. Shannon, Revised effective ionic radii and systematic studies of interatomie distances in halides and chaleogenides, Acta Crystallogr. A32 (1976) 751.
[27] J.C. Slater, Atomic radii in crystals, J. Chem. Phys. 41 (1964) 3199.
[28] J. Henney, N.A. Hill, D.T. Livey UKAEA (Harwell) Report AERE-R 4175 (1963).
[29] F.L. Oetting, J.D. Navratil, The chemical thermodynamic properties of nuclear materials: (II) High temperature enthalpy of uranium carbides, J. Nucl. Mater. 45 (1973) 271–283.
[30] M.G. Ferrier, B.C. Childs, C.M. Silva, M.M. Greenough, E.E. Moore, A.J. Swift, S. A. Di Pietro, A.A. Martin, J.R. Jeffries, K.S. Holliday, Unconventional pathways to carbide phase synthesis via thermal decomposition of UI_4(1,4-dioxane)$_2$, Inorg. Chem. 61 (2022) 17579–17589.
[31] P.E. Potter, The uranium-plutonium-carbon-oxygen systems, J. Nulc. Mater. 42 (1972) 1–22.
[32] G. Ervin, W.L. Korst, Note on the reported high-temperature solubility of uranium in uranium monocarbide, J. Nucl. Mater. 19 (1966) 193–195.
[33] P. Magnier, A. Accary, Carbides in Nuclear Energy, 1, Macmillan, 1964, p. 22.
[34] J.J. Norreys, Carbides in nuclear energy, ed. L. E. Russell et al. 1 (1964) 435.
[35] W. Chubb, Carbides in nuclear energy, Nucl. Sci. Eng. 22 (4) (1965) 500–501.
[36] J. Williams, R.A.J. Sambell, The uranium monocarbide-uranium mononitride system, J. Less-Common Met. 1 (1959) 217–226.
[37] W. Jander, Reactions in the solid state at higher temperatures. Reaction rates of endothermic reactions, Z. Anorg. Chem. 163 (1927) 1.
[38] T. Namba, T. Koyama, G. Imada, M. Kanno, M. Yamawaki, Kinetics of the carbothermic reduction of a $ThO_2 + UO_2 + C$ mixture to prepare (Th, U)C, J. Nucl. Mater. 150 (1987) 226–232.
[39] A. Boettcher, G. Schneider, in: Proceedings of the United Nations Atomic Energy Conference, Geneva 15, 1958, p. 964.
[40] J. Williams, Rev. mbt., 13 (1956) 189.
[41] L.M. Litz, A.B. Garrett, F.C. Croxton, Preparation and structure of the carbides of uranium, J. Am. Chem. Soc. 70 (1948) 1718.
[42] J. Williams, R.A.J. Sambell, D. Wilkinson, The variation of unit-cell edge of uranium monocarbide in arc melted uranium-carbon alloys, J. Less-Common Met. 2 (1960) 352–356.
[43] Y. Suzuki, Y. Arai, T. Sasayama, M. Handa, Mechanism of carbothermic reduction of (U, Pu)O_2 to (U, Pu)C, J. Nucl. Sci. Technol. 20 (10) (1983) 874–876.
[44] U.D. Wdowik, V. Buturlim, L. Havela, D. Legut, Effect of carbon vacancies and oxygen impurities on the dynamical and thermal properties of uranium monocarbide, J. Nucl. Mater. 545 (2021) 152547.
[45] W. Chubb, R.W. Getz, C.W. Townley, Diffusion in uranium monocarbide, J. Nucl. Mater. 13 (1964) 63–74.
[46] S.K. Mukerjee, J.V. Dehadraya, V.N. Vaidya, D.D. Sood, Kinetic study of the carbothermic synthesis of uranium monocarbide microspheres, J. Nucl. Mater. 172 (1990) 37–46.
[47] Y. Suzuki, Y. Arai, T. Sasayama, Carbothermic synthesis of uranium-plutonium mixed carbide, J. Nucl. Sci. Technol. 20 (7) (1983) 603–610.